# Generation of surface steps on Pt(977) induced by the catalytic oxidation of CO

O. Balmes, Geoffroy Prévot, X. Torrelles, E. Lundgren, S. Ferrer

▶ **To cite this version:**

O. Balmes, Geoffroy Prévot, X. Torrelles, E. Lundgren, S. Ferrer. Generation of surface steps on Pt(977) induced by the catalytic oxidation of CO. Journal of Catalysis, 2014, 309, pp.33-37. 10.1016/j.jcat.2013.09.001 . hal-01238948

**HAL Id: hal-01238948**

**https://hal.science/hal-01238948v1**

Submitted on 30 Apr 2020

**HAL** is a multi-disciplinary open access archive for the deposit and dissemination of scientific research documents, whether they are published or not. The documents may come from teaching and research institutions in France or abroad, or from public or private research centers.

L'archive ouverte pluridisciplinaire **HAL**, est destinée au dépôt et à la diffusion de documents scientifiques de niveau recherche, publiés ou non, émanant des établissements d'enseignement et de recherche français ou étrangers, des laboratoires publics ou privés.

Distributed under a Creative Commons Attribution 4.0 International License

# Generation of surface steps on Pt(977) induced by the catalytic oxidation of CO

O. Balmes [a], G. Prevot [b], X. Torrelles [c], E. Lundgren [d], S. Ferrer [c,e,*]

[a] ESRF, 6, rue Jules Horowitz, F-38043 Grenoble Cedex, France
[b] Institut des NanoSciences de Paris, UMR CNRS 7588, Université Pierre et Marie Curie-Paris 6, 4, Place Jussieu, 75005 Paris, France
[c] Institut de Ciència de Materials, CSIC, Bellaterra 08193, Spain
[d] Department of Synchrotron Radiation Research, Institute of Physics, Lund University, Box 118, S-221 00 Lund, Sweden
[e] ALBA Light Source, Carret. BP 1413, Cerdanyola del Valles 08290, Spain

The catalytic oxidation of CO has been investigated on the stepped Pt(977) surface at near ambient pressure and elevated temperature. It has been found that the reactivity is maximum at approximately the stoichiometric proportion of reactants and that surface monoatomic steps are generated by the reaction itself, being most abundant when the reaction proceeds with maximum efficiency.

## 1. Introduction

Atoms at surface steps have lower atomic coordination than regular surface atoms in flat terraces, and already in 1925 [1], they were proposed as possible active sites in surface chemical processes. The early papers from the Somorjai group [2] suggested that surface steps in Pt surfaces were active sites for C–C and C–H bond breaking. Further published literature provides a variety of examples of dissociation of molecules chemisorbed at step sites. To mention some, Xu et al. [3] observed with Infrared (IR) techniques that on Pt(335), dissociative adsorption of $O_2$ and CO occurred preferentially on the step sites. Zambelli et al. [4] demonstrated with STM that the dissociation of NO on Ru(0001) occurred at steps. Dahl et al. [5] reported from adsorption rate measurements and density functional calculations that the dissociation of $N_2$ on Ru(0001) occurs at the steps with much higher probability than on terraces. Also, IR measurements by Zubkov et al. [6] evidenced the dissociation of CO on Ru(109) steps, and Vang et al. [7] evidenced with STM measurements and calculations that steps are more efficient for C–C bond breaking than for C–H bond breaking when ethylene is adsorbed on Ni(111). The above examples illustrate that steps play a key role on the dissociative chemisorption of gas molecules. In most cases, the experimental support arises from UHV surface techniques.

Surface chemical reactions are intrinsically more complex than chemisorption processes since they involve additional elementary steps. This additional complexity blurs the precise role of steps in many cases. The intuitive idea that the presence of steps always increases the reactivity can be questioned. This is technically difficult to address since only a few techniques can provide direct structural information under reaction conditions. Already in the initial papers from the Somorjai group on the dehydrogenization of cyclohexane on stepped Pt surfaces, the authors observed that the maximum turnover frequency (TOF) did not occur on the surface with the highest density of steps [8]. Gland et al. [9] investigated under UHV the oxidation of CO on Pt(321) and concluded that atomic oxygen reacts with the CO adsorbed on the terraces more rapidly that with CO adsorbed on the steps. Ford et al. [10] investigated with thermal desorption spectroscopy, the adsorption of a variety of gases on several stepped surfaces and their generally concluded that their results did not support the ideas that surface steps and kinks have any effect on catalytic activity. Szabo et al. showed that CO adsorbed on the terraces was more effective in producing $CO_2$ than CO on the steps [11]. The same ideas were investigated in Pt nanoparticles supported on alumina by Atalik and Uner [12], which studied the oxidation of CO under UHV conditions and concluded that atoms at flat surfaces had higher activity per surface site than low coordinated edge or corner atoms. Experiments at atmospheric pressure by Silvestre-Albero et al. [13] on supported

* Corresponding author at: ALBA Light Source, Carret. BP 1413, Cerdanyola del Valles 08290, Spain.
*E-mail address:* ferrer@cells.es (S. Ferrer).

Pd catalysts on a hydrogenation reaction gave similar results. The reaction was found to be particle size independent for particles larger than, 4 nm which exhibit TOFs identical to Pd(1 1 1) single crystals. Similar results reported by Goodman [14] on the oxidation of CO at a pressure of a few torr on Pd nanoparticles did not reveal noticeable dependence of the $CO_2$ formation rate on the Pd cluster size. However, Au particles seem to be an exception since the results are opposite. As shown by Lopez et al. [15], low coordinated Au atoms were associated with high TOFs since small Au particles (2–4 nm) exhibited TOFs ~100 times larger than particles of 20–30 nm in size. Most published studies deal with the variation in the reaction rate for different densities of steps; however, the variation in the step density during the reaction has been much less investigated.

A previous paper by Hendriksen et al. [16] on the oxidation of CO to $CO_2$ on Pd(0 0 1) surfaces exposed to 500 mbar of $O_2$ and 25 mbar of CO investigated with surface X-ray diffraction *in operando* conditions, evidenced an oscillatory reaction rate and surface morphology. The surface was periodically changing from metallic to oxidized, and the production of $CO_2$ was also oscillating in phase with the structure of the surface. High reaction rates corresponded to oxide surfaces and low rates to metallic surfaces. The high reaction rate was associated with a broadening of the diffracted peaks indicating an increase in surface roughness that was interpreted as being due to an increase in the density of surface steps. From these observations, it was concluded that surface steps had a key role on the reactivity.

We report here new results on *in situ* CO oxidation experiments near atmospheric pressure on a vicinal Pt(9 7 7) surface, which consists of a periodic array of equally separated monatomic steps, where we have identified the role of the steps on the reaction rate not by measuring the evolution of the width of the diffracted peaks from the surface lattice as previously, but by monitoring the evolution of the intensities of the diffracted peaks arising from the step array itself. In our experiments, the partial pressures of CO and $O_2$ during the reaction were always kept outside of the self-sustained oscillatory regime described in Ref. [16].

In a few words, we found that the actual surface under reaction conditions is faceted and consists of (1 1 1) and (9 7 7) areas that have to coexist with rough or step bunched areas to keep the mean surface orientation. The maximum density of (9 7 7) areas and hence of atomic steps occurred when the reactants had the stoichiometric proportion (two COs per one $O_2$ molecule). Excess of CO or $O_2$ over the 2:1 nominal ratio in the gas mixture caused an increase in the proportion of (1 1 1) facets and a decrease in (9 7 7) revealing the disappearance of some monoatomic steps. If the gas proportion was returned back to the stoichiometric ratio, the (9 7 7) facet increased, i.e., steps were regenerated. This process was reversible.

In short, the reaction drives the morphology of the catalyst optimizing the density of monoatomic steps to maximize the rate.

## 2. Materials and methods

The Pt(9 7 7) sample was a disk of diameter 10 mm and thickness 3 mm obtained after cutting a single crystalline rod. Previous to the experiment, it was annealed to 1000 °C in air to recrystallize and to eliminate carbon impurities. Afterward, it was mounted on a thermally insulated ceramic heater which allowed reaching temperatures up to 900 °C as measured with a thermocouple in contact with the crystal. The crystal and heater were installed in a flow reactor previously described [17] connected to a UHV chamber allowing sputtering/annealing cycles for surface preparation. The reactants, CO and $O_2$, were introduced with a computer controlled gas manifold which allowed to precisely define their relative proportions. The partial flows were set at the entrance of the reactor, whereas the total pressure $P$ in the reactor, in the range 10–200 mbar, was set by a pressure controller at the exit. In this way, the ratio of the partial pressures of the reactants $R = P_{CO}/P_{O2}$ was determined and used as an experimental variable to describe the reaction conditions. $R = 2$ corresponds to the stoichiometric proportions of the reactants whereas $R > 2$ and $R < 2$ to CO and $O_2$ rich conditions, respectively. A leak from the reactor to a gas analyzer in the UHV chamber allowed monitoring the production of $CO_2$.

Concerning the reactivity of the sample, after it was mounted on the ceramic heater, the vacuum system was pumped down and baked to reach UHV pressures. This resulted in a contaminated sample that was inert and did not produce $CO_2$. To prepare a clean and reactive surface, we sputtered the front face of the crystal (the 9 7 7 face) with Ar ions, and later, we annealed the crystal to order the surface lattice. During ion sputtering, a fraction of the ion beam impinged on one side of the crystal, and from the total sputtered surface area, about 14% corresponded to the edge of the crystal which might contribute to the reactivity. In our analysis, this edge effect has been ignored. In addition, we have assumed that the back side of the crystal was unreactive since it was in close contact with the ceramic heater. Also, in previous experiments, the reactivities of the vessel, sample holder, and heater were measured and found to be negligible.

The turnover frequencies have been estimated with two methods: measuring the partial pressure of the produced $CO_2$ and measuring the temperature increase in the sample due to the exothermic heat of reaction with the appropriate calibration of the thermal characteristics of the sample heater. The sample was near adiabatic conditions due to the isolating sample heater. Within a factor two to three, both methods agreed which is considered acceptable due several experimental uncertainties.

The reactor chamber was installed on a diffractometer at the Surface Diffraction beamline (ID3) at ESRF [18]. Seventeen keV X-rays passing through the Be dome of the reactor impinged the crystal surface at a grazing angle of 1–2°. Diffracted intensities were collected with a 2D maxipix pixel detector from ESRF while rotating the sample as required to sweep the reciprocal space. We described the fcc crystal lattice with an orthogonal basis adapted to our vicinal surface: $A = (-7, 9/2, 9/2)a_0$, $B = (0, -1/2, 1/2)a_0$, $C = (9, 7, 7)a_0$, $\alpha = \beta = \gamma = 90°$, $a_0 = 0.3924$ nm (see Fig. 1a). The corresponding $H, K, L$ coordinates are used to index reflections in reciprocal space. As an example, the (1 1 1) reflection in conventional reciprocal units has $(H,K,L) = (0,2,23)$. In this basis, the diffuse lines of diffracted intensity perpendicular to the surface and parallel to the $L$ axis in reciprocal space which are designed as crystal truncation rods (CTR) [19] have even values of $H + K$.

Fig. 1 panel a illustrates the definitions of the vectors **A** and **C** and a schematic drawing of the stepped surface. Panel b shows a portion of the $H$–$L$ plane (at $K = 0$) of reciprocal space and the corresponding diffracted intensities. In addition to the Bragg reflections from the bulk of the crystal which have the largest intensities, the diffuse streaks (CTRs) of intensity emanating from the Bragg reflections and parallel to the $L$ axis are evident. They are fingerprints of the 9 7 7 plane at the surface. The inclined streak of intensity in the figure arises from 1 1 1 surface facets. The coexistence of stepped and 1 1 1 surface areas was also reported previously on Pt(9 9 7) and attributed to trace impurities or intrinsic thermal instability [20].

## 3. Results and discussion

Setting $P = 200$ mbar and the stoichiometric proportions of the reactants ($P_{CO}/P_{O2} = 2/1$) which corresponds to $R = 2$, while heating the sample from room temperature to 200 °C did not produce any

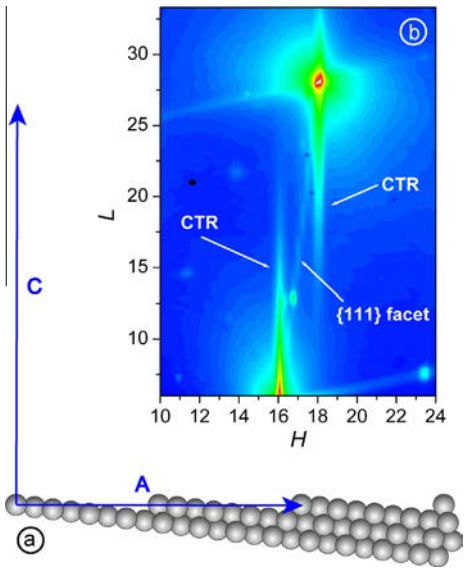


**Fig. 1.** (a) Side view of the 977 surface and representation of the **A** and **C** vectors in direct space. **C** is perpendicular to the 997 planes and **A** has a length twice the step separation. (b) Diffracted intensities in a portion of the plane $(H,L)$ at $K = 0$ in reciprocal space. The $H$ and $L$ axes are parallel to vectors **A** and **C** respectively. The intense red spot at $(H,L) = (18,28)$ arises from a Bragg reflection from the bulk of the crystal. The diffuse intensity streak emanating from the Bragg reflection, parallel to the $L$ axis, is a crystal truncation rod (CTR) of the 977 surface plane. At $(H,L) = (16,5)$ there is another Bragg reflection which tail is visible in the lower part of the figure. Again, its associated diffraction rod from the stepped surface parallel to the $L$ axis is noticeable. In addition, an inclined diffuse intensity line connecting the two bulk Bragg reflections is visible. It corresponds to a diffracted rod from 111 surface planes indicative of the existence of surface 111 facets. (For interpretation of the references to color in this figure legend, the reader is referred to the web version of this article.)

increase in the partial pressure of $CO_2$ in the background of the UHV chamber which was in the mid $10^{-9}$ mbar range. Above 200 °C, the $CO_2$ production started to be detectable and increased exponentially with the temperature (see Fig. 2a). The corresponding apparent activation energy is 27 kcal/mol which is very close to the one found on Pt(111) and Pt(112) for similar pressure conditions [21], but lower than the activation energy found for $O_2$ rich conditions on Pt(111) [22]. Such high energy indicates that CO desorption is the limiting step in this regime [23]. Around 390 °C, a change occurs and the TOF shows a plateau which corresponds to a mass transfer limited regime. The vertical dashed line in Fig. 2a results from the intersection of a straight line in the Arrhenius plot with slope of 27 kcal/mol and a horizontal line trough the plateau.

If the gas ratio was maintained to stoichiometric ($R = 2$), no variation in the diffraction signal from the surface was observed. However, if the relative partial pressures of the reactants were varied, pronounced modifications of the diffraction signal were observed. Several scans performed along the $H$ direction at $T \approx 490$ °C are presented in Fig. 3. The initial curve, obtained after 2 h at this temperature for a fixed value $R = 2$, exhibits a broad peak at $H = 9$, from the step periodicity, and a sharp central peak at $H = 8.15 \pm 0.05$, which arises from the (111) facets. If $R$ was diminished to 1.3 (oxygen rich mixture, red curve), the (111) facet peak increased and the (977) step peak diminished strongly. If then $R$ was set to 19 (very rich CO mixture, black curve), the (111) facet peak still increased and the (977) step peak completely disappeared. Setting again $R = 2$ caused the (111) facet peak to decrease and the reappearance of the (977) step peak (blue curve, after 80 min at $R = 2$). The vicinal surface became better ordered than at the beginning since an additional step peak showed up at $H = 7$ [24].

Referring to the topmost scan in Fig. 3, the full widths at half maximum $\Delta H$ of the (111) and step peaks are approximately 0.1 and 0.5. We may estimate the surface correlation lengths of the (111) facets and (977) areas evaluating $\mathbf{A}/\Delta H$ (**A**: lattice vector see Section 2 and Fig. 1) [25] which results in 177 Å and 35 Å, respectively. At $R = 19$ and 1.3, the values for the (111) facets are 256 and 201 Å, respectively.

These variations in the surface morphology were accompanied with variation in the TOF evidenced by the pressure of $CO_2$ and the sample temperature. As an example, the drop in surface temperature when $R$ was varied from 2 to 19 was of 40 °C. The maximum TOF was observed around $R = 2.0$ with a rather symmetric behavior below and above that value. For $R > 2$ (CO rich gas mixture), the reactivity decreases due to a lower $O_2$ entrance flux and also to the fact that the surface is poisoned with CO preventing oxygen adsorption. For $R < 2$ (oxygen rich gas mixture) oxygen induced faceting and limited supply of CO also cause a drop in the TOF.

Further insight into the relationship surface morphology and reactivity is shown in Fig. 4, which displays the temporal dependence of the diffracted intensities (bottom part) of the (977) step peak at $H = -23$ and the peak from the (111) facets at $H = -22.7$ and the corresponding values of $R$ (top part). The surface temperature was ~420 °C. The step peak has significant intensity when $R$ is very close to 2.0. Values of $R$ above or below 2.0 originate an enhancement of the intensity of the (111) facets and a decrease in that of the (977) steps. When $R$ was increased from 1.9 to 2.0 (time ≅ 11,500 s), the step peak reappeared and the facet peak diminished.

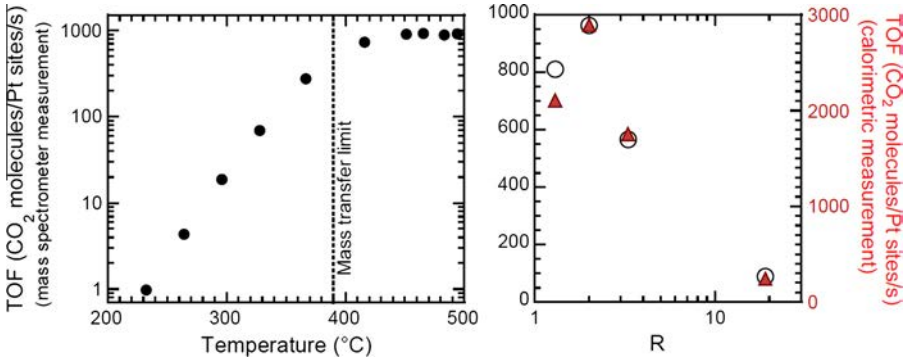


**Fig. 2.** Measured turnover frequencies (TOFs) for 200 mbar of total pressure of $CO + O_2$ Left panel. TOF as a function of the temperature of the Pt sample for a fixed stoichiometric proportion $R = P_{CO}/P_{O2} = 2/1$. Right panel. TOFs for different stoichiometries from $O_2$ rich ($R = 1.5$) to CO rich ($R = 19$) gas mixtures for $T \cong 490$ °C. TOFs are either derived from mass spectrometer (black symbols, left vertical axis) or from calorimetric measurements (red symbols, right vertical axis). (For interpretation of the references to color in this figure legend, the reader is referred to the web version of this article.)

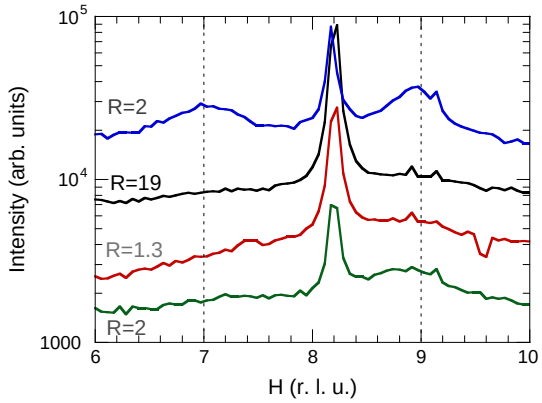


**Fig. 3.** Diffracted intensities vs. $H$ at fixed $K = 1$ and $L = 4$ values. The measurements were performed under 200 mbar CO + $O_2$ at $T \cong 490$ °C. Bottom and topmost curves: the proportion of CO and $O_2$ was adjusted to the stoichiometric $P_{CO}/P_{O2} = 2/1$ value ($R = 2$). Red and black curves correspond to oxygen rich ($R = 1.3$) and CO rich ($R = 19$) gas mixtures respectively. The broad peaks at $H = 7$ and 9 (dashed vertical lines) are fingerprints of the monoatomic steps. These peaks disappear when the gas mixture is not stroichiometric. The central peak at $H = 8.2$ arises from 1 1 1 surface facets. The curves have been shifted vertically for clarity. (For interpretation of the references to color in this figure legend, the reader is referred to the web version of this article.)

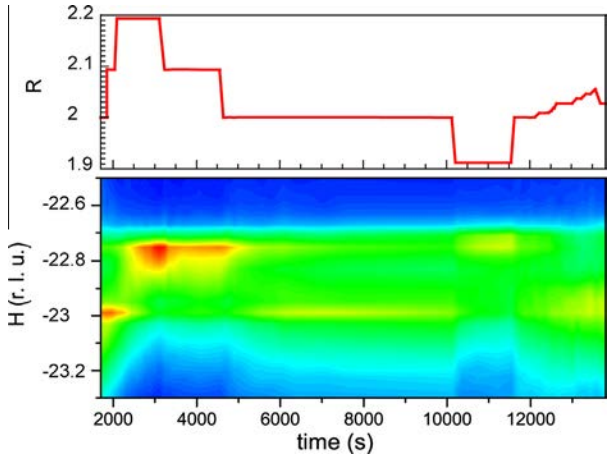


**Fig. 4.** Top panel: The $CO/O_2$ gas mixture was varied as a function of time around its stroichiometric 2/1 value ($R = P_{CO}/P_{O2} = 2$). Starting with a stoichiometric mixture, it was changed to $R = 2.2$ at $t \cong 2200$ s (CO rich mixture) in two steps and subsequently it was set again to the stoichiometric $R = 2$ value at $t \cong 5000$. At $t \cong 10{,}000$ s the gas mixture was changed to $O_2$ rich ($R = 1.9$) and finally was set again to the stoichiometric proportion followed by very small changes to a slightly CO rich mixture. Bottom panel: Temporal evolution of the diffracted intensity while the changes displayed in the top panel were being carried out. The plot corresponds to a series of H scans similar to those displayed in Fig. 3 but taken in another portion of reciprocal space. Here $K$ and $L$ are fixed at 1 and 8 respectively while $H$ is varied. The intensity $H = -23$ arises from the surface monoatomic steps. The color code ranging from blue to red denotes increasing intensities. The intensity at $H \cong -22.7$ arises from 1 1 1 surface facets. At the start of the experiment, the intensity from the monoatomic steps is pronounced and it fades out when the gas mixture is made CO rich while the intensity from the facets that was initially low clearly develops. When the gas mixture is set back to the stoichiometric proportion (near $t = 5000$ s) the intensity from the step increases again while that of the facet strongly decreases. Subsequent change to an oxygen rich mixture ($t \cong 10{,}000$ s) decreases again the intensity from the steps in favor of the facets. Finally, the intensity from the steps reappears when the gas mixture is returned to the stoichiometric value. The linear color scale ranges from (2.8 to 6.4) $\times 10^4$ photons/s (red is most intense). (For interpretation of the references to color in this figure legend, the reader is referred to the web version of this article.)

The results displayed in Fig. 4 indicate that the stability range of the surface morphology is narrow: $R = 2 \pm 0.05$ approximately. The value $\Delta R = 0.05$ allows to estimate the maximum tolerable departure of the reactant partial pressures from the stoichiometric values which do not cause a change on the step density. The experimental setup causes that the effective partial pressures $P_{CO}^{surf}$, $P_{O_2}^{surf}$ and $P_{CO_2}^{surf}$ seen by the surface may strongly differ from the nominal partial pressures at the inlet of the reactor $P_{CO}^{inl}$ and $P_{O_2}^{inl}$ [26]. For $R \approx 2$, the surface environment is mostly $CO_2$, since both CO and $O_2$ react immediately at the surface. We may assume that $P_{O_2}^{surf} \approx P_{CO}^{surf} \approx 0$ due to mass transfer limitations through the $CO_2$ gas environment. For $R > 2$, oxygen immediately reacts at the surface and $P_{O_2}^{surf}$ remains zero, but $P_{CO}^{surf}$ does not, since there is not enough $O_2$ for reacting with the CO molecules at the surface. For small pressure variations, we assume that the extra CO pressure at the inlet directly adds to the surface partial pressure $\Delta P_{CO}^{surf} \approx \left(P_{CO}^{inl} - 2P_{O_2}^{inl}\right) = P_{Tot}^{inl}(R-2)/(1+R)$ where $P_{Tot}^{inl} = P_{CO}^{inl} + P_{O_2}^{inl}$. Then, for $R = 2 + \Delta R$ $\Delta P_{CO}^{surf} \approx P_{Tot}^{inl}\Delta R/3$. For $R < 2$, the symmetric situation occurs and $\Delta P_{O_2}^{surf} \approx P_{Tot}^{inl}\Delta R/6$.

As $P_{Tot}^{inl} = 200$ mbar, we obtain $\Delta P_{CO}^{surf} = 3.3$ mbar and $\Delta P_{O_2}^{surf} = 1.7$ mbar as the maximum tolerable deviation pressures.

What is most remarkable, in our view, is the fact that the maximum TOF is associated with a maximum of monoatomic steps. This indicates that the activation barrier of the catalytic reaction diminishes when the density of monoatomic steps increases which clearly illustrates the important role of the steps in the reaction kinetics and that the decrease in free energy which drives the reaction induces a restructuring of the morphology of the catalyst to speed it up.

Concerning the exact surface structure during the maximum TOF, a number of scenarios may be proposed. The formation of an oxide (2D or 3D) would result in an increased roughening of the surface [16], which is not observed during maximum TOF in the present investigation. Instead, we observe a well-ordered (9 7 7) surface under maximum TOF, showing that the substrate surface steps are instrumental for the reaction and not the oxide steps from a resulting Pt oxide. Furthermore, for Pt(3 3 2), evidence for a 1D oxide decorating the monatomic steps was proposed based on photoemission under UHV conditions [27], and it was shown that this oxidic oxygen was able to react more easily with CO than oxygen chemisorbed on the Pt terraces. Such a 1D-oxide along the step edges would not alter the (9 7 7) periodicity as probed in the present investigation. In addition, previously published work [28] shows that on Rh(1 1 1) oxidized atoms at the edges of the oxide islands act as a supply of oxygen in the oxidation of CO. Therefore, we propose that our observation on the enhanced reactivity associated with the presence of steps could be due to a higher concentration of 1D "step-oxide" which acts as an intermediate reaction species providing oxygen to the CO molecules.

## 4. Conclusions

1. Under reaction conditions near atmospheric pressure, the Pt surface is faceted and consist of (9 7 7) and (1 1 1) regions.
2. The density of monoatomic steps, monitored by the intensity of the diffracted peaks arising from the periodic step array, is maximum when the reactants have the stoichiometric proportions. Under these conditions, the reactivity of the surface is maximum.
3. Departure of stoichiometry reduces the density of monoatomic steps that can be recovered by setting back the stoichiometric proportions.

## Acknowledgments

The technical assistance of H. Isern, L. Petit and T. Dufrane is highly appreciated.

## References


[1] H.S. Taylor, Proc. Roy. Soc. Lond. A 108 (1925) 105.
[2] D.W. Blakely, G.A. Somorjai, J. Catal. 42 (1976) 181.
[3] J. Xu, J.T. Yates Jr., J. Chem. Phys. 99 (1993) 725.
[4] T. Zambelli, J. Wintterlin, J. Trost, G. Ertl, Science 273 (1996) 1688.
[5] S. Dahl, A. Logadottir, R.C. Egeberg, J.H. Larsen, I. Chorkendorff, E. Törnqvist, J.K. Nørskov, Phys. Rev. Lett. 83 (1999) 1814.
[6] T. Zubkov, G.A. Morgan Jr., J.T. Yates Jr., O. Kuhlert, M. Lisowski, R. Schillinger, D. Fick, H.J. Jansch, Surf. Sci. 526 (2003) 57.
[7] R.T. Vang, K. Honkala, S. Dahl, E. Vestengaard, J. Schnadt, E. Laegsgaard, B.S. Clausen, J.K. Norskov, F. Besenbacher, Nat. Mater. 4 (2005) 160.
[8] S.M. Davies, G.A. Somorjai, Surf. Sci. 91 (1980) 73.
[9] J.L. Gland, M.R. McClellan, F. Read McFeely, J. Chem. Phys. 79 (1983) 6349.
[10] L.P. Ford, H.L. Nigg, P. Blowers, R.I. Masel1, J. Catal. 179 (1998) 163.
[11] A. Szabó, M.A. Henderson, J.T. Yates, J. Chem. Phys. 96 (1992) 6191.
[12] B. Atalik, D. Uner, J. Catal. 241 (2006) 268.
[13] J. Silvestre-Albero, G. Rupprechter, H. Freund, J. Catal. 266 (2009) 359.
[14] D.W. Goodman, J. Catal. 216 (2003) 213.
[15] N. Lopez, T.V.W. Janssens, B.S. Clausenb, Y. Xu, M. Mavrikakis, T. Bligaard, J.K. Nørskov, J. Catal. 223 (2004) 232.
[16] B.L.M. Hendriksen, M.D. Ackermann, R. van Rijn, D. Stoltz, I. Popa, O. Balmes, A. Resta, D. Wermeille, R. Felici, S. Ferrer, J.W.M. Frenken, Nat. Chem. 2 (2010) 730.
[17] R. van Rijn, M.D. Ackermann, O. Balmes, T. Dufrane, A. Geluk, H. Gonzalez, H. Isern, E. de Kuyper, L. Petit, V.A. Sole, D. Wermeille, R. Felici, J.W.M. Frenken Rev, Sci. Instrum. 81 (2010) 014101.
[18] S. Ferrer, F. Comin, Rev. Sci. Instrum. 66 (1995) 1674.
[19] I.K. Robinson, Phys. Rev. B 33 (1986) 3830.
[20] E. Hahn, H. Schief, V. Marsico, A. Fricke, K. Kern, Phys. Rev. Lett. 72 (1994) 3378.
[21] L. Piccolo, S. Nassreddine, F. Morfin, Cat. Tod. 189 (2012) 42.
[22] X. Su, P.S. Cremer, Y.R. Shen, G.A. Somorjai, J. Am. Chem. Soc. 119 (1997) 3994.
[23] T. Engel, G. Ertl, Advances in Catalysis, Academic Press, 1979, pp. 1–78.
[24] The peaks of the steps in Fig. 3 exhibit some small displacements respect to their nominal positions at $H = 9$ and 7 due to some uncorrected small drifts of the sample position producing small misalignments as a consequence of the changes in experimental parameters.
[25] E. Vlieg, J.F. Van Der Veen, S.J. Gurman, C. Norris, J.E. Macdonald, Surf. Sci. 210 (1989) 301.
[26] S. Matera, K. Reuter, Phys. Rev. B 82 (2010) 085446.
[27] J.G. Wang, W.X. Li, M. Borg, J. Gustafson, A. Mikkelsen, T.M. Pedersen, E. Lundgren, J. Weissenrieder, J. Klikovits, M. Schmid, B. Hammer, J.N. Andersen, Phys. Rev. Lett. 95 (2005) 256102.
[28] E. Lundgren, J. Gustafson, A. Resta, J. Weissenrieder, A. Mikkelsen, J.N. Andersen, L. Köhler, G. Kresse, J. Klikovits, A. Biederman, M. Schmid, P. Varga, J. Electron Spectrosc. Related Phenomena 144–147 (2005) 367.